REPORT DOCUMENTATION PAGE

Form Approved OMB NO. 0704-0188

1. REPORT DATE (DD-MM-YYYY)	2. REPORT TYPE	3. DATES COVERED (From - To)
	New Reprint	-

4. TITLE AND SUBTITLE

High frequency magneto-dielectric effects in self-assembled ferrite-ferroelectric core-shell nanoparticles

5a. CONTRACT NUMBER
W911NF-12-1-0545

5b. GRANT NUMBER

5c. PROGRAM ELEMENT NUMBER
611102

6. AUTHORS

G. Sreenivasulu, M. Popov, V. M. Petrov, F. A. Chavez, G. Srinivasan

5d. PROJECT NUMBER

5e. TASK NUMBER

5f. WORK UNIT NUMBER

7. PERFORMING ORGANIZATION NAMES AND ADDRESSES

Oakland University
2200 N. Squirrel Rd

Rochester, MI 48309 -4402

8. PERFORMING ORGANIZATION REPORT NUMBER

9. SPONSORING/MONITORING AGENCY NAME(S) AND ADDRESS (ES)

U.S. Army Research Office
P.O. Box 12211
Research Triangle Park, NC 27709-2211

10. SPONSOR/MONITOR'S ACRONYM(S)
ARO

11. SPONSOR/MONITOR'S REPORT NUMBER(S)
62336-MS.17

12. DISTRIBUTION AVAILIBILITY STATEMENT

Approved for public release; distribution is unlimited.

13. SUPPLEMENTARY NOTES

The views, opinions and/or findings contained in this report are those of the author(s) and should not contrued as an official Department of the Army position, policy or decision, unless so designated by other documentation.

14. ABSTRACT

Magneto-dielectric effects in self-assembled core-shell nanoparticles of nickel ferrite (NFO) and barium titanate (BTO) have been investigated in the millimeter wave frequencies. The core-shell nano-composites were synthesized by coating 100 nm nickel ferrite and 50 nm barium titanate nanoparticles with complementary coupling groups and allowing them to self-assemble in the presence of a catalyst forming heterogeneous nanocomposites. Magneto-electric (ME) characterization of as-assembled particles has been carried out by measurements of the relative permittivity μ_r as a function of frequency f under an applied static magnetic field H over 16-24 GHz

15. SUBJECT TERMS

Core-shell nanoparticles, self-assembly, ferrite, ferroelectric, magnetoelectric

16. SECURITY CLASSIFICATION OF:			17. LIMITATION OF ABSTRACT	15. NUMBER OF PAGES	19a. NAME OF RESPONSIBLE PERSON
a. REPORT	b. ABSTRACT	c. THIS PAGE			Gopalan Srinivasan
UU	UU	UU	UU		19b. TELEPHONE NUMBER: 248-370-3419

Report Title

High frequency magneto-dielectric effects in self-assembled ferrite-ferroelectric core-shell nanoparticles

ABSTRACT

Magneto-dielectric effects in self-assembled core-shell nanoparticles of nickel ferrite (NFO) and barium titanate (BTO) have been investigated in the millimeter wave frequencies. The core-shell nano-composites were synthesized by coating 100 nm nickel ferrite and 50 nm barium titanate nanoparticles with complementary coupling groups and allowing them to self-assemble in the presence of a catalyst forming heterogeneous nanocomposites. Magneto-electric (ME) characterization of as-assembled particles has been carried out by measurements of the relative permittivity ?r as a function of frequency f under an applied static magnetic field H over 16-24 GHz. Measurements show an H-induced decrease in ?r of 1 to 1.5%. But a giant magneto-dielectric effect with an H-induced change in permittivity as high as 28% is measured under dielectric resonance in the samples. A strong ME coupling was also evident from H-tuning of dielectric resonance in the composites. A theory for the high frequency magneto-dielectric effect has been developed and consists of the following steps. First the Bruggeman model is used to estimate the effective dielectric constant for the shell consisting of the BTO particles and voids considered as spherical air-pores. Then the permittivity for the core and shell is estimated taking into consideration the sample porosity. Finally the H-dependence of the permittivity due to ME interactions is calculated from the free energy considerations. Estimated ?r vs. H and dielectric resonance frequency vs. H characteristics are in general agreement with the data.

REPORT DOCUMENTATION PAGE (SF298)
(Continuation Sheet)

Continuation for Block 13

ARO Report Number 62336.17-MS
High frequency magneto-dielectric effects in sel...

Block 13: Supplementary Note

Approved for public release; distribution is unlimited.

AIP Advances

High frequency magneto-dielectric effects in self-assembled ferrite-ferroelectric core-shell nanoparticles

M. Popov, G. Sreenivasulu, V. M. Petrov, F. A. Chavez, and G. Srinivasan

Citation: AIP Advances **4**, 097117 (2014); doi: 10.1063/1.4895591
View online: http://dx.doi.org/10.1063/1.4895591
View Table of Contents: http://scitation.aip.org/content/aip/journal/adva/4/9?ver=pdfcov
Published by the AIP Publishing

AIP ADVANCES **4**, 097117 (2014)

High frequency magneto-dielectric effects in self-assembled ferrite-ferroelectric core-shell nanoparticles

M. Popov,[1,2] G. Sreenivasulu,[1] V. M. Petrov,[3] F. A. Chavez,[4] and G. Srinivasan[1,a]

[1]*Physics Department, Oakland University, Rochester, MI 48309-4401, USA*
[2]*Radiophysics Department, Taras Shevchenko National University of Kyiv, Kyiv, 01601, Ukraine*
[3]*Institute of Electronic and Information Systems, Novgorod State University, Veliky Novgorod 173003, Russia*
[4]*Chemistry Department, Oakland University, Rochester, MI 48309-4401, USA*

(Received 26 June 2014; accepted 1 September 2014; published online 10 September 2014)

Magneto-dielectric effects in self-assembled core-shell nanoparticles of nickel ferrite (NFO) and barium titanate (BTO) have been investigated in the millimeter wave frequencies. The core-shell nano-composites were synthesized by coating 100 nm nickel ferrite and 50 nm barium titanate nanoparticles with complementary coupling groups and allowing them to self-assemble in the presence of a catalyst forming heterogeneous nanocomposites. Magneto-electric (ME) characterization of as-assembled particles has been carried out by measurements of the relative permittivity ε_r as a function of frequency f under an applied static magnetic field H over 16–24 GHz. Measurements show an H-induced decrease in ε_r of 1 to 1.5%. But a giant magneto-dielectric effect with an H-induced change in permittivity as high as 28% is measured under dielectric resonance in the samples. A strong ME coupling was also evident from H-tuning of dielectric resonance in the composites. A theory for the high frequency magneto-dielectric effect has been developed and consists of the following steps. First the Bruggeman model is used to estimate the effective dielectric constant for the shell consisting of the BTO particles and voids considered as spherical air-pores. Then the permittivity for the core and shell is estimated taking into consideration the sample porosity. Finally the H-dependence of the permittivity due to ME interactions is calculated from the free energy considerations. Estimated ε_r vs. H and dielectric resonance frequency vs. H characteristics are in general agreement with the data. [http://dx.doi.org/10.1063/1.4895591]

I. INTRODUCTION

A composite of ferromagnetic and ferroelectric phases is a multiferroic in which the coupling between the electric and magnetic subsystems is aided by mechanical strain.[1–6] The magneto-electric (ME) interaction in the composite is a product property, i.e., magnetostriction in an applied magnetic field resulting in piezoelectric charge generation. Studies so far have focused primarily on composites with ferromagnetic/ferrimagnetic metals, alloys or oxides and ferroelectrics such as barium titanate (BTO), lead zirconate titanate (PZT), and lead magnesium niobate-lead titanate (PMN-PT).[1–15] Efforts on thick film, thin film, and bulk composites involved measurements of sample response to an applied magnetic field H, termed direct-ME effect, or to an applied electric field E called converse-ME effect. For direct-ME effect one measures the induced polarization, voltage or change

[a]Author to whom correspondence should be addressed. Electronic mail: srinivas@oakland.edu.

in permittivity due to H. Studies on converse-ME effect in general involve measurements of induced magnetization, permeability or magnetic anisotropy field due to E.[1–15] Several composites were reported to show very strong ME coupling at low frequencies and resonance enhancement of ME interactions at frequencies corresponding to bending, longitudinal and thickness acoustic modes.[1–6]

The magneto-dielectric effect (MDE) involves studies on the influence of an applied magnetic field on the dielectric constant of a material.[16–25] It is a powerful tool for investigations on the nature of direct-ME effects in single phase and composite multiferroics. There have been several reports in recent years on the observation of MDE due to phase transitions in single phase multiferroics[16–19] or magnon-phonon coupling in antiferromagnets.[21,22] But there have been very few reports on the observation and modeling of MDE in composite multiferroics. In a composite with ferromagnetic La-Sr-manganite and a ferroelectric, the strain mediated ME coupling was reported to show 9.5% change in the permittivity under H = 9 T.[23] Modeling efforts on MDE in composites so far include thermodynamic formalisms based on the Landau-Devonshire theory applied to cobalt particles dispersed in barium titanate (BTO) matrix[24] and a non-linear thermodynamic approach to estimate the magneto-capacitance effect in BTO or PZT films on substrates of ferromagnetic alloys.[25]

This work is on the observation and theory of MDE in multiferroic nanocomposites. The ME coupling in nanostructures analogs of bulk and layered multiferroic composites is of interest since one anticipates strong strain mediated coupling due to a large surface-to-volume ratio. Nanostructures of core-shell particles, pillars in a host matrix, coaxial tubes and wires have been studied in recent years.[26–35] The strength of ME coupling in these systems was studied by several techniques including piezo force microscopy and magnetic force microscopy.[35–37] Theories predict strong ME coupling in these systems.[26] The nanocomposites can be further assembled into superstructures by surfactant-assisted or magnetic field or electric directed assembly techniques.[33,34] Due to electric polarization and magnetic dipole moment associated with the nanostructures it is possible to obtain rings, chains, bundles, and two-dimensional and three-dimensional periodic arrays of the composites for investigations on ME interactions and for useful technologies.[33]

Here we report on measurements and theory of millimeter-wave magneto-dielectric effects in chemical assemblies of NFO-BTO core-shell particles. We synthesized these core-shell nanocomposites by coating the ferroic nanoparticles with complementary coupling groups and allowing them to self-assemble.[38–41] We employed BTO (diameter = 50 nm) and NFO (diameter = 100 nm) nanoparticles for the assemblies. One of the nanoparticles, BTO or NFO, was functionalized azide groups and the other with alkyne groups.[41] Following this, the functionalized particles were heterogeneously linked together in the presence of a Cu(I) catalyst via the "click" reaction forming heterogeneous nanocomposites.[39–41] The core-shell structure was confirmed with electron microscopy and magnetic force microscopy. The magnetic and ferroelectric nature of the composites was confirmed with magnetization, ferromagnetic resonance and polarization P vs. E measurements. Magneto-electric characterization of as-assembled particles was carried out by high frequency magneto-dielectric effects. The studies involved measurements of the relative permittivity ε_r as a function of frequency f under an applied static magnetic field H over 16-24 GHz. With appropriate choice for sample dimensions two frequency regions were investigated. (i) A region that is free of dielectric resonance in the sample: A decrease in ε_r was measured under H with a fractional change in ε_r of 1 to 1.5% for H = 4 kOe. (ii) The frequency range that overlaps the dielectric resonance: A giant magneto-dielectric effect with an H-induced change in permittivity as high as 28% was measured. A strong ME coupling was also evident from H-tuning of dielectric resonance in the composites.

The first model for MDE in self-assembled core-shell particulate composites is also discussed here. The theory is done in 3 steps. First we use the Bruggemann's effective medium model to estimate the permittivity of the shell with BTO particles and by considering the shell porosity as air-pores. Second, the effective permittivity of sample of core-shell particle is estimated taking into consideration the sample porosity. Third, the free energy formalisms of the Landau-Devonshire theory is used to describe the ME couplings between strain and order parameters and the resulting change in the permittivity. Our theory predicts a decrease in the permittivity in H. The variation in the permittivity results from changes in equilibrium strain components and, therefore, equilibrium polarization in applied magnetic fields due to magnetostrictive coupling. Theoretical ε_r

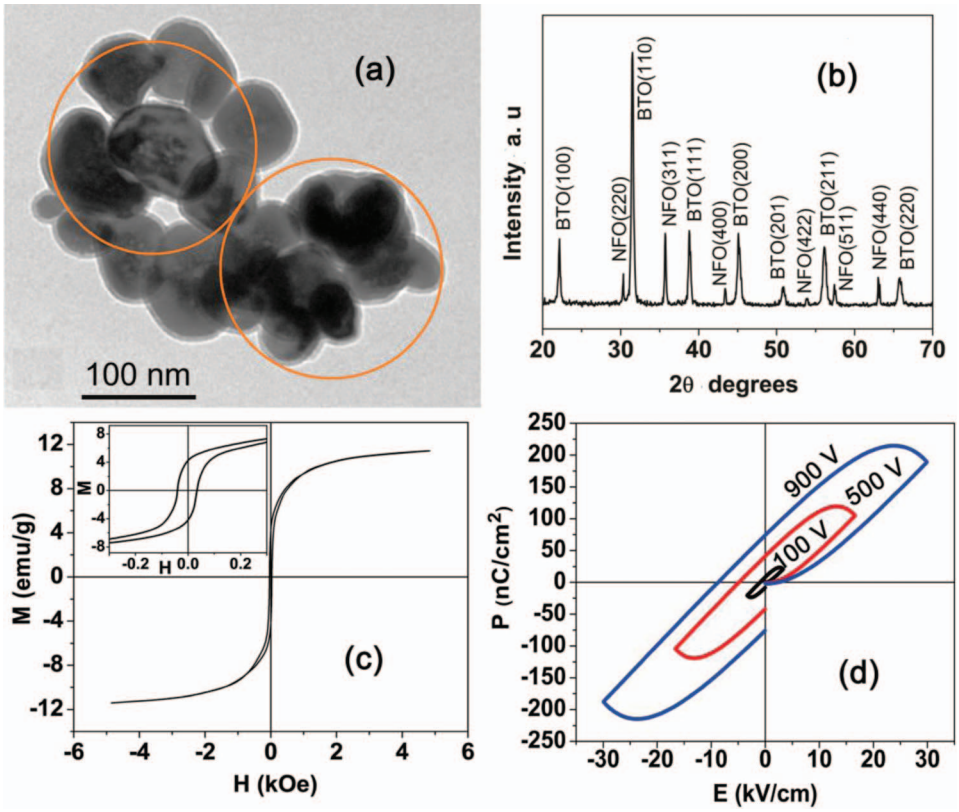

FIG. 1. (a) TEM micrograph showing core-shell structures for chemically assembled clusters with 100 nm nickel ferrite (NFO) core and 50 nm barium titanate (BTO) shell. (b) X-ray diffraction data for as-assembled core-shell particles. (c) Room temperature magnetization as a function of static magnetic field H for the clusters. (d) Polarization vs. E for the NFO-BTO core shell composites.

vs. H and dielectric resonance frequency vs. H characteristics are in general agreement with the data.

II. EXPERIMENT

Core-shell particles consisting of 100 nm diameter nickel ferrite, $NiFe_2O_4$ (NFO) core and 50 nm barium titanate $BaTiO_3$ (BTO) shell were synthesized and used in this study. The self-assembly procedure is discussed in detail in Ref. 41 and involved following 3 steps. (i) Preparation of NFO particles by co-precipitation techniques (vendor supplied BTO was used). (ii) Functionalizing the particles with two complementary coupling groups, one with azide groups and the other with alkyne groups. Azide modification of nanoparticles and functionalization with alkyne group by attaching *O*-propargyl citrate was conformed using FTIR (KBr pellet) spectroscopy.[40] (iii) The generation of hetero-assemblies between nanoparticles was effected by Cu(I)-catalyzed azide-alkyne cycloaddition (CuAAC) reaction (commonly known as "click" chemistry).[38–41]

Sample characterization in terms of structure, composition, and ferroic order parameters are detailed in Ref. 41. Here we summarize important findings. Structural and compositional studies on as-assembled particles were carried out by scanning and transmission electron microscopy (TEM), X-ray diffraction, and scanning probe microscopy. TEM micrograph in Fig. 1(a) shows approximately 6 to 8 particles of BTO in a shell around the NFO core. One expects eight 50 nm-BTO particles around the 100 nm-NFO core in 2*D* and 16 BTO particles around NFO in 3*D*. The X-ray diffraction (XRD) pattern is shown in Fig. 1(b). The data shows diffraction peaks expected for NFO and BTO and the composites were free of any impurity phases. The chemical composition of the clusters was

confirmed with energy dispersive x-ray spectroscopy. Magnetic characterization of as-assembled clusters was performed by magnetization and ferromagnetic resonance. Room-temperature data on magnetization M vs. H (measured with a Faraday Balance) for dried powder of the composite are shown in Fig. 1(c). The sample shows ferromagnetic behavior with hysteresis and remnance and the magnetization compared favorably with reported value for polycrystalline nickel ferrites.[42] Ferromagnetic resonance measurements over 8-16 GHz showed a broad absorption. Ferroelectric characterization involved measurements of P vs. E. Representative data (obtained with a Radiant Ferroelectric Tester) for pressed discs of as-assembled powders are shown in Fig. 1(d). A relatively small remnant polarization and coercive field compared to bulk BTO are measured for the core-shell particulate composite. Further details on structural, magnetic and ferroelectric characterization are provided in Ref. 41.

This report focuses on the nature of ME interactions in the nanocomposites by magneto-dielectric effect, i.e., the magnetic field induced variation in the permittivity of the nanocomposite. The effect was investigated from 16 to 24 GHz with an Agilent vector network analyzer. The transmission line method used involves placing a sample of appropriate shape inside a rectangular waveguide or coaxial airline.[43] Waveguide fixtures are band-limited but operate at higher frequencies than coaxial airline and require a rectangular sample. A precision quarter-wavelength WR-42 waveguide section was used as the sample holder. Dried as-assembled composite powder was pressed into a pellet so as to completely fill the cross section of the waveguide without gaps at the fixture walls. Samples of dimensions 10.7 mm × 4.3 mm and thickness in the range 0.43 to 0.55 mm were used. The waveguide with the sample was excited with microwave power and a two-port measurement of transmission and reflection coefficients were done to estimate the complex permittivity. During the measurements a bias static magnetic field was applied along the wide wall of waveguide, and dielectric constant variation with frequency and H was recorded for H = 0 - 5 kOe. Upper bound for H was determined from the condition that FMR frequency should be below the waveguide cut-off frequency.[41]

III. MAGNETO-DIELECTRIC EFFECTS: RESULTS AND DISCUSSION

First we measured the real part of the relative permittivity ε_r' vs f over 16–18 GHz on a sample of dimensions 10.7 mm × 4.3 mm × 0.55 mm. The specific thickness was chosen in order to eliminate any dielectric resonance in the sample. Data on the frequency dependence of ε_r' in a static magnetic field H are shown in Fig. 2. The permittivity remains almost constant with increasing f. With the application of H, ε_r' is found to decrease with increasing H. Figure 2 shows the fractional change in the permittivity $\Delta\varepsilon_r'/\varepsilon_r'(0) = [\varepsilon_r'(H) - \varepsilon_r'(H=0)] / \varepsilon_r'(H=0)$ for H = 4 kOe. It ranges from −1% to −1.5%. But a giant magneto-dielectric effect, with an H-induced change in ε_r' by 28%, was observed under dielectric resonance in the sample as discussed next.

Investigations on MDE at dielectric resonance in the composites are of importance since the resonance frequency is a function of the dielectric constant. Thus any H-induced changes in ε_r' are directly reflected as a change in resonance frequency. A sample of dimensions 10.7 mm × 4.3 mm and a thickness of 0.43 mm was used. Data on ε_r' vs f for a series of H over the range 16–24 GHz are shown in Fig. 3. A resonance is clearly seen in the data and is due to dielectric resonance in the sample of core-shell nanocomposite. With the application of H, a general decrease in ε_r' is observed except for a narrow frequency range extending from 19 to 20 GHz over which ε_r' is found to increase with increasing H. The fractional change in the dielectric constant for H = 4 kOe is shown in Fig. 4. For frequencies away from the resonance region one measures 1 to 5% decrease in ε_r', while at resonance the dielectric constant increases by 23%. Thus a giant magneto-dielectric effect in the core-shell particulate composite with a 28% net change in permittivity is evident in the data of Fig. 4.

For measurements of the dielectric mode frequencies f_r we obtained profiles of the imaginary part of the permittivity ε_r'' as a function of f. Such ε_r'' vs. f profiles for a series of H are shown in Fig. 5. An increase in the resonance frequency f_r with increasing H is seen in Fig. 5. Data on H-dependence of f_r for the composite are shown in Fig. 5. The mode frequency f_r increases from 19.3 GHz for H = 0 to 20 GHz for H = 5 kOe. The shift in f_r with H could be attributed to the

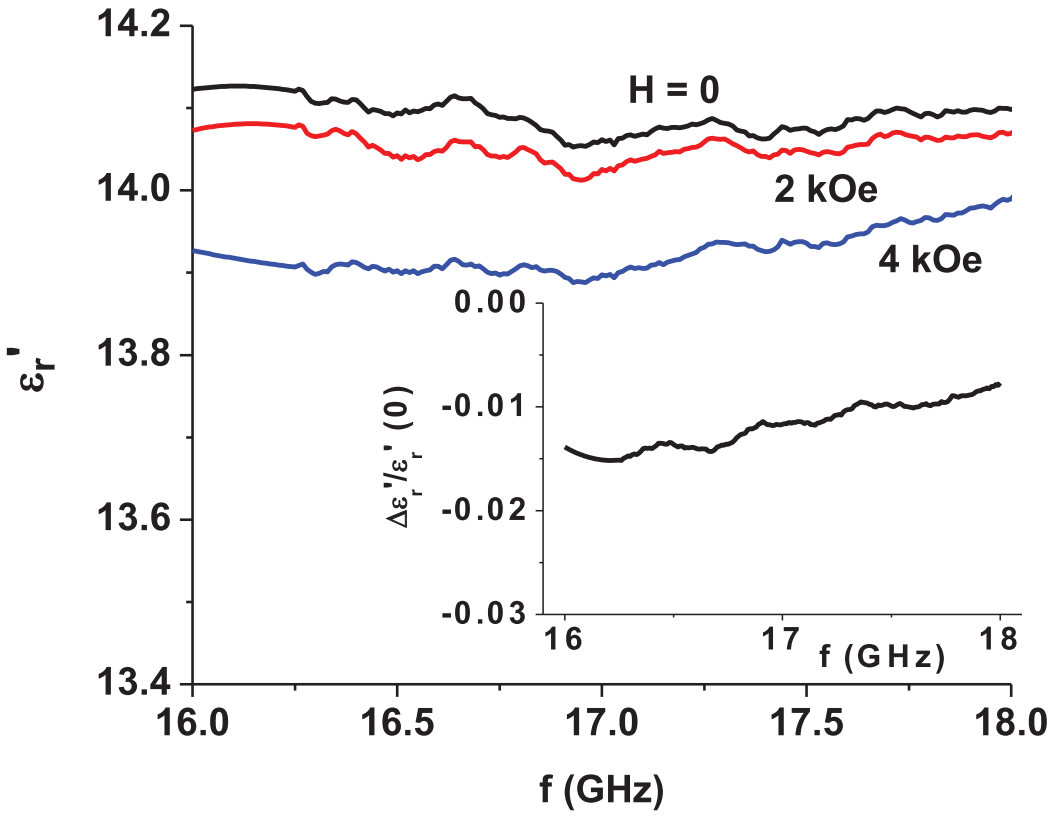

FIG. 2. Frequency dependence of the real part of the relative permittivity ε_r' as a function of static field H measured on as-assembled NFO-BTO composite. The inset shows the fractional change in ε_r' vs. f.

change in the permittivity that arises due to strain mediated ME coupling in the composite. But one also expects variations in f_r due to any change in the composite permeability. It has previously been observed for a dielectric resonator of pure nickel ferrite that f_r initially decreases with increasing H.[44] The initial decrease in f_r takes place due to changes in the permeability as the bias field was increased from 0 to saturation field H_{sat}, while for $H>H_{sat}$, the frequency begins to increase. For the data in Fig. 5 only an increase in f_r vs H is observed with no initial decrease. Thus the decrease in permittivity with H in the composite completely compensates the down-shift in f_r due to any change in the permeability. It should be noted that the primary cause for the increase in f_r with H is the decrease in permittivity due to strain mediated ME effects as will be inferred by the theory discussed in the following section.

Now we compare the MDE in the as-assembled core-shell ferrite-ferroelectric composites with similar studies on single phase multiferroics. The MDE in single phase multiferroics are generally associated with H induced magnetic phase transitions that result in an induced polarization and a change in the permittivity and is on the order of 1% or less in fields of several Tesla.[5] Thus the off-resonance MDE on the order of 1 to 1.5% for H = 4 kOe in the present system is much stronger than in single phase multiferroics. But there are also reports of a giant MDE in single phase materials under H due to magnetic field induced phase transitions.[16–19,45,46] Past reports on MDE in nano-composites include studies on core-shell nanoparticles of BTO and $ZnFe_2O_4$.[47] Dielectric constant measured at 1 MHz showed a 1.3% change for H = 1 T. Similar studies were reported on nanopyramids of PZT of diameter 50–100 nm dispersed in a cobalt ferrite matrix. Magneto-capacitance in the system showed a 1.46% increase in H.[48] Although there have been very few studies on MDE under dielectric resonance in composites, a giant MDE was reported recently under electromechanical resonance in PZT-Terfenol-D layered composites.[49] A static field H was found to tune the frequency of acoustic modes in the sample, resulting in a large change in ε.

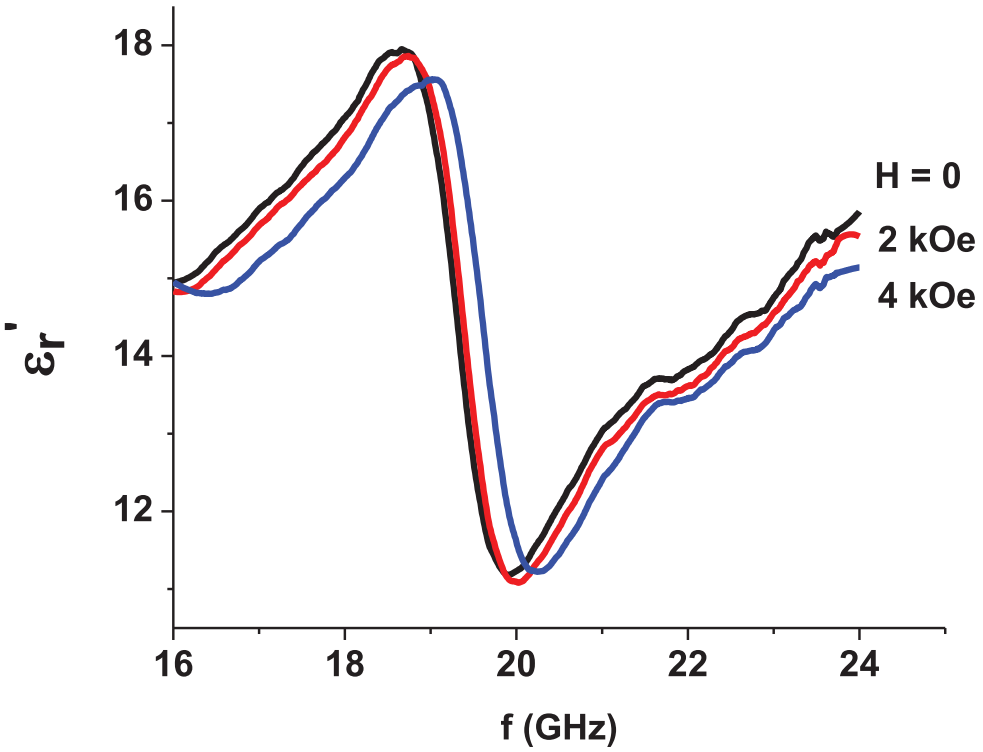

FIG. 3. Data on ε_r' vs. f for a series of H for a pressed sample of as-assembled NFO-BTO core shell composite. The sample dimension was chosen so that dielectric resonance mode is present in the sample in the above frequency range.

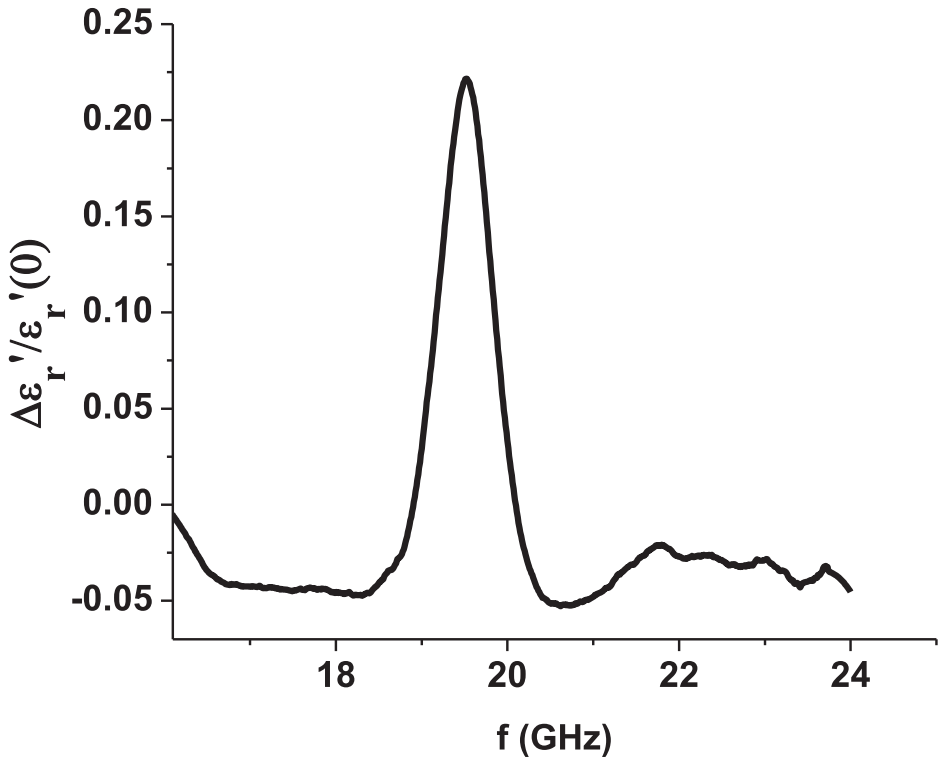

FIG. 4. Fractional change in ε_r' in H = 4 kOe as a function of f estimated from the data in Fig. 3.

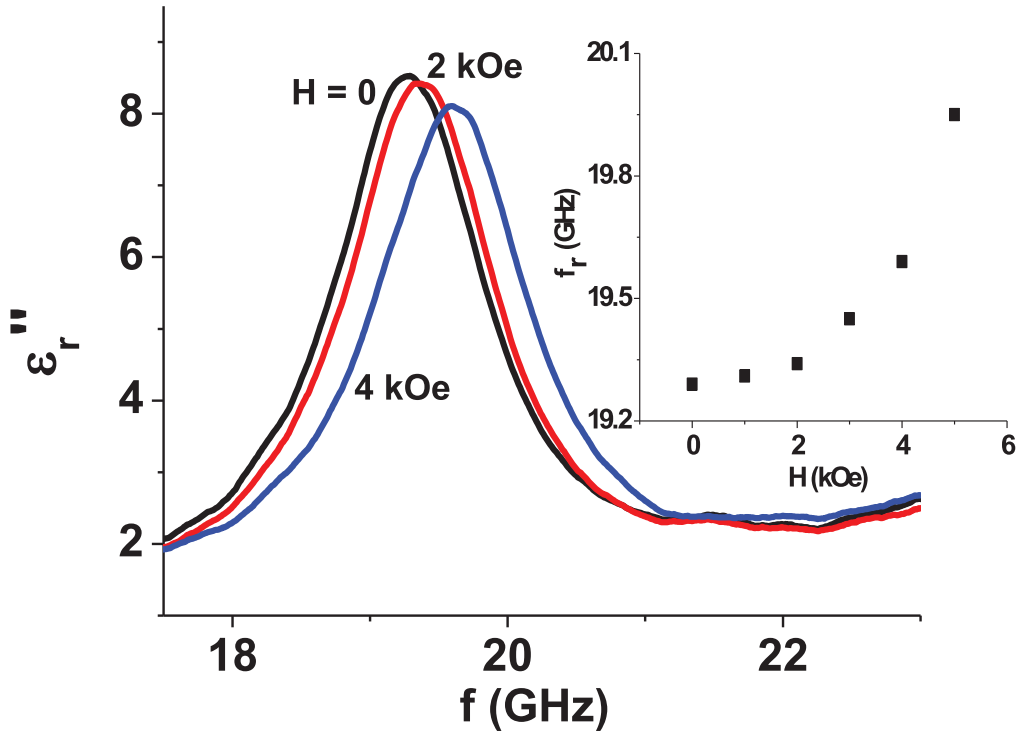

FIG. 5. Profiles of the imaginary part of the relative permittivity ε_r'' vs f for a series of H for the tangentially biased core-shell particulate composites. The inset shows the H-dependence of the dielectric resonance frequency f_r.

The data in Fig. 5 on H-tuning of dielectric resonance clearly demonstrate the utility of the technique for measurements of the strength of ME interactions in the core-shell composite. This procedure is analogous to E-tuning of FMR in ferromagnetic-ferroelectric composites for studies on strength of converse-ME effects.[1,5,6] Data in Fig. 5 could be used to estimate the strength of direct-ME coupling. Defining the ME coupling strength as $A = \delta f_r$ / H where δf_r is the shift in the resonance frequency for applied field H, one obtains $A = 140$ MHz/kOe. This DME strength should be compared with CME coupling strength A ranging from 1 MHz cm/kV for hexaferrite-PZT to 970 MHz cm/kV for FeGaB/PZN-PT.[10,11] The CME in ferrite-ferroelectric bilayers also formed the basis for a new class of high frequency signal processing devices such as resonators, filters and phase shifters. A similar device application, H-tunable dielectric resonators, phase shifters, or isolators could be envisioned for dielectric resonance in the core-shell composites.[50] Such device use also would require efforts directed at reduction of the line-width for the resonance in Fig. 5.

IV. THEORY AND DISCUSSION

Next we discuss models for (i) the magneto-dielectric effects in the core-shell composites for frequencies away from dielectric resonance and (ii) H-tuning of the dielectric resonance. The off-resonance MDE is considered first. Various models in the past considered the effective dielectric response of heterogeneous mixtures in terms of permittivity, volume fractions, and geometry of the initial components.[51–53] The formulae provided in these reports are based on distinct structure of a mixture; therefore the validity is determined by how closely the models describe the actual structure. In this work, a model for the dielectric response of the NFO-BTO core-shell structure and its variation with applied magnetic field is discussed. Two types of porosity, in the shell occupied by BTO particles and in the compacted pellet of the sample, must be taken into account in the estimates of permittivity. Assuming the BTO particles in the shell to be perfectly spherical, one estimates a porosity of 26% for the shell. The porosity in the compacted disk of the sample is 30%

in our case. For finding the effective parameters of porous sample, we consider it as a structure consisting of core-shell matrix with embedded 50 nm diameter spherical air-pores. To provide a suitable description of the dielectric behavior of the sample, a three-phase mixture (core+ porous shell+porous sample) model is needed. One of the most commonly used dielectric mixture theories is the Bruggeman effective-medium theory.[51,52] According to this model that takes into account depolarization effects, the constituents of the mixture are considered as spherical particles dispersed in a background medium. Bruggeman theory enables one to avoid the uncertainty connected to the choice of background medium that is inherent in the Maxwell-Garnett treatment.[53] The Bruggeman model was found to accurately predict the dielectric constants of two-phase dielectric mixtures in a wide range of compositions.

To estimate the effective dielectric constant of the core-shell system a two step approach was used. First, the effective medium theory based on Clausius–Mossoti equation was used to determine the effective dielectric constant of the shell (with BTO particles and air- pores). Second, the dielectric constant of the whole sample with the core, shell and pores in the sample is determined. We also take into account the frequency dependence of dielectric constant. According to the well-known Clausius-Mossotti equation, for a structure with background medium of permittivity ε_b containing n_i numbers of spherical inclusions per unit volume:

$$\frac{\varepsilon_{eff} - \varepsilon_b}{\varepsilon_{eff} + 2\varepsilon_b} = \sum_{i=1}^{N} \frac{n_i a_i}{3\varepsilon_b} \tag{1}$$

where ε_{eff} is effective dielectric constant of the whole structure, a_i is polarizability of i-inclusion. First we consider the shell with spherical BTO (i = 1) and air-pores (i = 2) inclusions. Then we assume two types of inclusions in the disk sample, core and porous shell of BTO (i = 1) and air-pores in the sample (i = 2), embedded in an effective medium generated by them.

For a concentric spherical core-shell particle embedded in a background medium of permittivity ε_b, Sihvola calcu1ated the polarizability by solving Laplace's equation in the spherical coordinates with the boundary conditions that the potential and the normal displacement vectors must be continuous at the boundaries between the particles and the surrounding medium.[54] Applying the solution to core-shell system leads to the following expression for polarizability[52]

$$a = 4\pi\varepsilon_b \frac{(\varepsilon_1 - \varepsilon_b)r_1^3 + (2\varepsilon_1 + \varepsilon_b)\left[(\varepsilon_2 - \varepsilon_1)r_2^3 + (2\varepsilon_2 + \varepsilon_1)/(\varepsilon_2 + 2\varepsilon_1) + 2(\varepsilon_2 - \varepsilon_1)r_2^3\right]}{(\varepsilon_1 + 2\varepsilon_b) + 2(\varepsilon_1 - \varepsilon_b)r_1^{-3}\left[(\varepsilon_2 - \varepsilon_1)r_2^3 + (2\varepsilon_2 + \varepsilon_1)/(\varepsilon_2 + 2\varepsilon_1) + 2(\varepsilon_2 - \varepsilon_1)r_2^3\right]} \tag{2}$$

where ε_1, ε_2, r_1 and r_2 are dielectric constants and radii of the shell and core, respectively. For an individual BTO particle, air-pore in the shell or air-pore in the sample in a background medium the polarizability can be approximated to that of a homogeneous sphere of radius r_3 in amedium and is given by

$$a = 4\pi\varepsilon_b r_3^3 \frac{\varepsilon_3 - \varepsilon_b}{\varepsilon_3 + 2\varepsilon_b} \tag{3}$$

with ε_3 and r_3 denoting the permittivity and radius of a sphere. Since the dielectric constant of the effective medium and the background medium are assumed to be equal in the Bruggeman model, the effective dielectric constant of the porous shell is calculated from Eq. (1) assuming $\varepsilon_b = \varepsilon_{eff}$ and taking into account Eq. (3). One may assume the dielectric constant of NFO to be a constant since its relaxation frequency is very high.[42] The frequency dependence of dielectric constant for BTO particles is taken into account by using the Debye equation

$$\varepsilon_1' = \frac{\varepsilon_s'}{1 + \left(\omega/\omega_r\right)^2} \tag{4}$$

where $\varepsilon_s' \sim 1300$[55] and $\omega_r \sim 750$ GHz[56] are the real part of static permittivity and dielectric relaxation frequency. In the discussion to follow, we denote the real part of permittivity by the symbol ε_1. Then the effective dielectric constant of the core-shell system is estimated from solution of Eq. (1) taking into account Eqs. (3) and (4). The estimated permittivity of shell with 50 nm BTO and spherical

air-pores (of diameter 50 nm) $\varepsilon_{1eff}/\varepsilon_0 = 610$ and for the compacted disk with particles of NFO core-BTO shell and 30% spherical air-pores in the sample the estimated value of $\varepsilon_{eff}/\varepsilon_0 = 15.2$. Calculations are for f = 18 GHz. It should be noted that using Eq. (1) implies neglecting the interparticle interactions since they are weak compared to intraparticulate ones.

Next we consider the static magnetic field dependence of the dielectric constant. The applied magnetic field gives rise to a change in dielectric response of the ferroelectric (FE) shell due magnetostrictive and electrostrictive coupling. To estimate the magnetically induced variation of dielectric constant, the structure can be treated as an assembly of spheres of the same diameter with no magnetic exchange interaction between adjacent particles. Each sphere is considered to be in single magnetic and ferroelectric domain state. The total free energy density of a ferromagnetic-ferroelectric core-shell particle is expressed by

$$F = vF^p + (1 - v)F^m \tag{5}$$

with F^p, F^m and v being the free energy densities of the ferromagnetic (FM) core and FE shell, and FE phase volume fraction, respectively. The free energy of the FE shell is the electrostrictive energy F_{es}

$$F^p = F_{es} \tag{6}$$

where $F_{es} = -{}^pq_{jkl}{}^pS_j P_k P_l$ with ${}^pq_{jkl}$, ${}^pS_k$, P_i and P_j denoting the electrostriction coefficients, strain tensor components, and polarization components. Similarly, the free energy of the FM core is equal to

$$F^m = F_m + F_H + F_{ms} + F_{dm}, \tag{7}$$

where F_m, F_H, F_{ms}, and F_{dm} are the ferromagnetic bulk free energy, energy in an magnetic field, magnetostriction energy, and magnetostatic energy, respectively. Magnetic energy components are defined as: $F_H = -HMcos\ \psi$ with H, M and ψ denoting the angle between the magnetic field and magnetization, and $F_{es} = -{}^mb_{ikl}{}^mS_iM_kM_l$, with ${}^mb_{ikl}$ and ${}^mS_i$ being the magnetoelastic coefficients and strain tensor component. Magnetic dipole interaction energy is defined by $F_{md} = \frac{\mu_0}{8\pi}\sum_{i\neq j}\left[\frac{(\vec{M}_i\cdot\vec{M}_j)}{r_{ij}^3} - \frac{3(\vec{M}_i\cdot\vec{r_{ij}})(\vec{M}_j\cdot\vec{r_{ij}})}{r_{ij}^5}\right]$ with M_i and M_j denoting the magnetic moments of magnetic particles. To simplify analysis of the complex problem of the magnetostatic interactions between the particles in the sample, we will use an effective magnetostatic energy density as a combination of the limiting cases of an isolated particle with demagnetization tensor N and a homogeneously magnetized ellipsoidal sample with the demagnetization tensor N',[57] $F_{md} = \frac{\mu_0(1-m)}{2}M\cdot N\cdot M + \frac{\mu_0 m}{2}M\cdot N'\cdot M$, where $N_1 = N_2 = N_3 = 1/3$ and m is the volume packing fraction of magnetic particles in the sample. The first limiting case of an isolated particle is obtained for $m \to 0$, the second one for $m = 1$.

The stress in the ferrite phase is assumed to be produced by applied magnetic field and transferred to ferroelectric shell. Strain and stress tensor components can be calculated by solving the elastostatic equations. This problem is similar to that of a spherical inclusion in a surrounding uniform medium.[58,59] Expressions for determining the stress components in the shell due to magnetostrictive coupling in the core are reduced to

$${}^pS_2 = {}^pS_1 = \frac{-24B}{y^5} + \left(\frac{4(5-4^pv)C}{3(1-2^pv)} + 2A\right)\frac{1}{y^3};$$

$${}^pS_3 = \frac{48B}{z^5} + \left(\frac{8(5-4^pv)C}{3(1-2^pv)} - 2A\right)\frac{1}{y^3};$$

$$A = \frac{Tr_2^3[(-1-{}^pv+2^mv)^p\mu + (1-2^pv+{}^mv)^m\mu + 2^pv^mv({}^p\mu - {}^m\mu)]}{6^p\mu(1+{}^pv)[(2-4^mv)^p\mu + (1+{}^mv)^m\mu}; \tag{8}$$

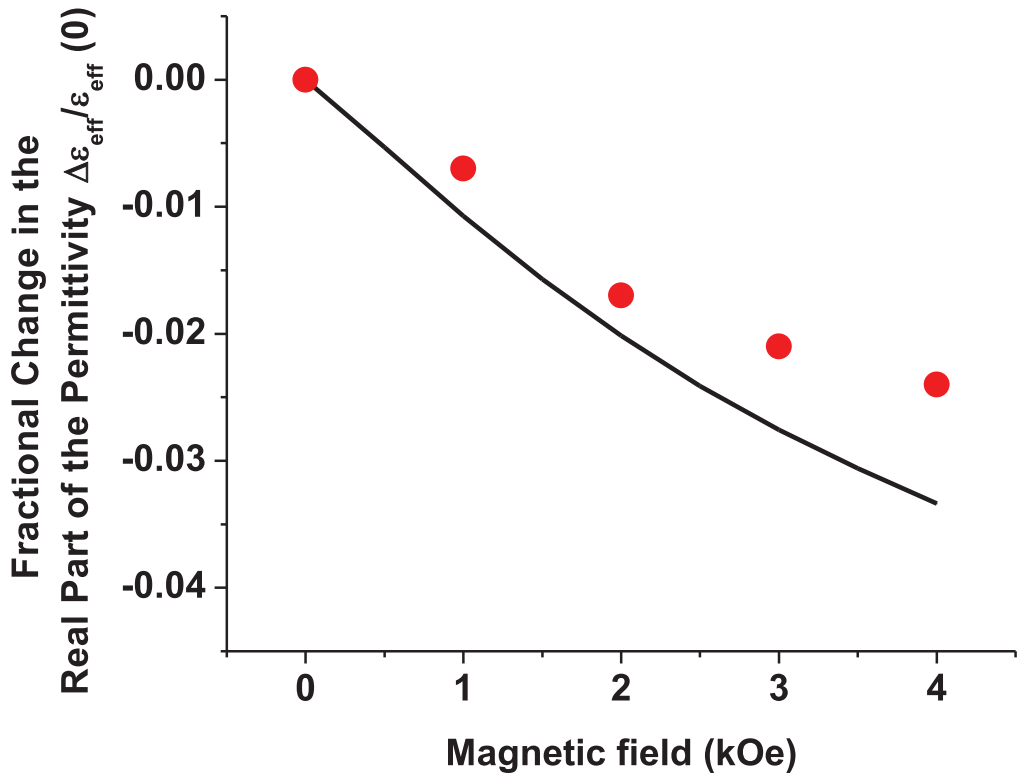

FIG. 6. Estimated static field H dependence of fractional variation in the real part of the permittivity for a disk sample of particles of 100 nm NFO core-50 nm BTO shell. The measured values from the data of Fig. 2 are shown for comparison.

$$B = \frac{Tr_2^5({}^p\mu - {}^m\mu)}{8^p\mu[(7-5^p\nu)^p\mu + (8+10^p\nu)^m\mu}; \qquad C = \frac{5Tr_2^3({}^p\mu - {}^m\mu)(1-2^p\nu)}{8^p\mu[(7-5^p\nu)^p\mu + (8+10^p\nu)^m\mu},$$

where μ and ν are elastic shear modulus and Poisson's ratio, y and z are measured relative to the origin at the core center and $T = {}^m b_{33} M_3{}^2$.

The estimated values of strain components should be substituted into Eq. (5) for free energy density that enables obtaining the equilibrium orientation of magnetization of the core using the condition $\frac{\partial F}{\partial \psi} = 0$. Then the magnetically induced change in shell polarization can be found from condition for minimum of free energy density $\frac{\partial F^p}{\partial P} = 0$. Taking into account the symmetry of core-shell structure, the total average equilibrium polarization can be assumed to be parallel to Z-axis. Finally, we find variation of the dielectric constant for the shell

$$\frac{\Delta\varepsilon_{33}}{\varepsilon_0} = \frac{1}{\varepsilon_0 V}\int_V \left(\frac{\partial^2 F^p}{\partial P_3^2}\right)^{-1} dV + 1, \tag{9}$$

with V being the shell volume. Based on Eq. (9), we obtained $\Delta\varepsilon_{33}/\varepsilon_0$ as a function of H and then calculated the fractional change in the effective dielectric constant ε_{eff} for the whole sample using Eqs. (1)–(3). The variation of the effective dielectric constant $\Delta\varepsilon_{\text{eff}}/\varepsilon_{\text{eff}}(0) = [\varepsilon_{\text{eff}}\,(\text{H}) - \varepsilon_{\text{eff}}\,(\text{H}=0)] / \varepsilon_{\text{eff}}\,(\text{H}=0)$ for the sample is shown in Fig. 6 as a function of H and compared with the data. The estimates are for BTO volume fraction of 74%, shell porosity of 26% and sample porosity of 30%. Decrease in permittivity in applied magnetic field can be accounted for by mechanical coupling on the boundaries between the ferroelectric and ferromagnetic phases due to electrostriction and

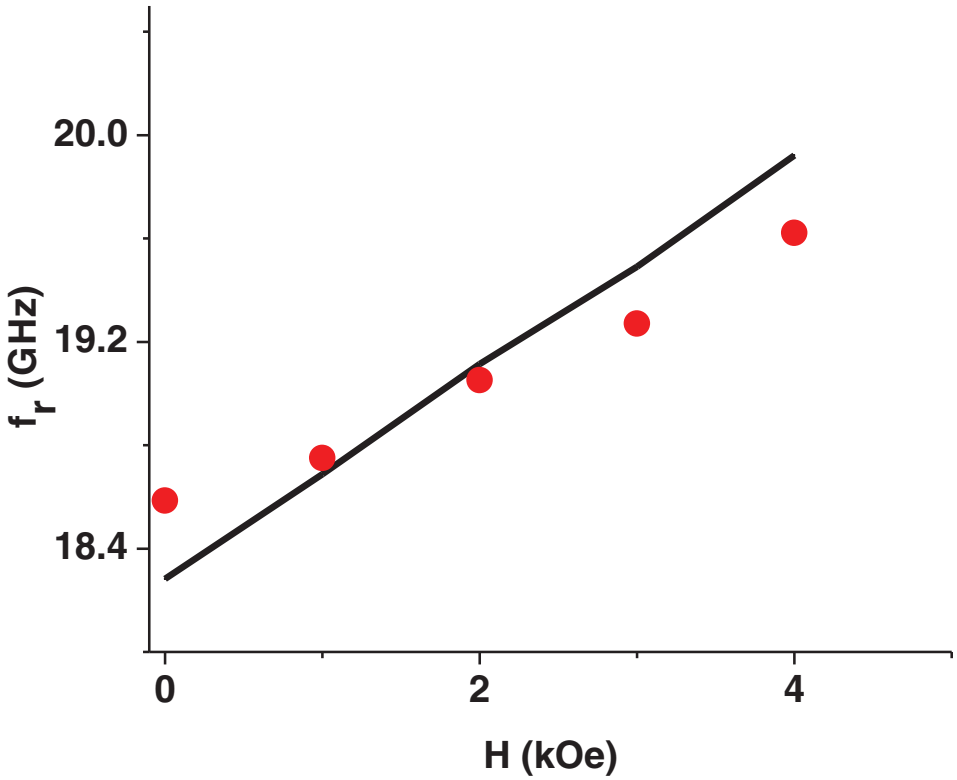

FIG. 7. Theoretical dielectric resonance frequency f_r as a function of static field H for the tangentially biased core-shell composite. Measured f_r from the data of Fig. 5 are shown for comparison.

magnetoelastic energy that enter Eq. (1). As mentioned above, boundary conditions consist of equating the displacement and stress components on the boundaries. Magnetic field gives rise to variation in equilibrium strain components and therefore equilibrium polarization. There is very good agreement between the measured and estimated values.

Next we discuss the observed change in dielectric mode frequency with applied magnetic field for the composite. The sample in the rectangular waveguide can be treated as a transmission line resonator.[60] The wavelength of the propagating waveguide mode is given by[60]

$$\lambda = \frac{1}{\sqrt{\frac{f^2}{c^2}\varepsilon\left(\mu - \mu_a^2/\mu\right) - \left(\frac{1}{2a}\right)^2}}$$

where μ and μ_a are the elements of magnetic permeability tensor, ε is the dielectric permittivity, and a is the length of the internal broad side of the waveguide. The dielectric resonance will take place at frequencies for which the sample thickness S is a multiple of half wavelength: $S = n\lambda/2$, $n = 1, 2, 3....$ Our calculations show that observed resonance corresponds to $n = 2$. The calculated f_r vs H dependence is presented in Fig. 7. The estimates are based on measured $\varepsilon(H)$ from Fig. 6, saturation magnetization $4\pi M_0 = 400$ G, gyromagnetic ratio $\gamma = 3.1$ MHz/Oe, and sample thickness $S = 0.43$ mm. There is very good agreement between theory and data.

V. CONCLUSIONS

The nature of mechanical strain mediated magneto-electric interactions has been investigated in self-assembled core-shell nanoparticles of nickel ferrite and barium titanate. Measurements of the real (ε_r') and imaginary (ε_r'') parts of the relative permittivity have been carried out over 16–24 GHz with rectangular platelets of samples of as-assembled powder in waveguides and from data on transmission and reflection coefficients of microwave power through the waveguide. The

ME coupling is found to result in 1 to 1.5 % decrease in ε_r' at 16–18 GHz for a nominal field of 4 kOe. A giant magneto-dielectric effect characterized by 28% change in ε_r' due to H is observed under dielectric resonance in the sample. The static magnetic field induced variation in ε_r' is found to influence the dielectric resonance with an increase in f_r by 140 MHz/kOe. A model is developed for the high frequency MDE. Estimated off-resonance ε_r' vs H and the static field dependence of the dielectric resonance frequency are in general agreement with the data.

ACKNOWLEDGMENTS

The research was supported by a grant from the Army Research Office (grant no: W911NF1210545). The efforts were also supported in part by grants from the National Science Foundation (DMR-0902701, ECCS-MRI- 1337716, CHE-0748607, CHE-0821487).

[1] Ce-Wen Nan, M. I. Bichurin, S. Dong, D. Viehland, and G. Srinivasan, J. Appl. Phys. **103**, 031101 (2008).
[2] Y. Yang, S. Priya, J. Li, and D. Viehland, J. Am. Ceram. Soc. **92**, 1552 (2009).
[3] J. Ma, J. Hu, Z. Li, and C. W. Nan, Adv. Mater. **23**, 1062 (2011).
[4] L. W. Martin and R. Ramesh, Acta Materialia **60**, 2449 (2012).
[5] G. Lawes and G. Srinivasan, J. Phys. D: Appl. Phys. **44**, 243001 (2011).
[6] N. X. Sun and G. Srinivasan, SPIN **2**, 1240004 (2012).
[7] Peng Zhao, Zhenli Zhao, Dwight Hunter, Richard Suchoski, Chen Gao, Scott Mathews, Manfred Wuttig, and Ichiro Takeuchi, Appl. Phys. Lett. **94**, 243507 (2009).
[8] Enno Lage, Frederik Woltering, Eckhard Quandt, and Dirk Meyners, J. Appl. Phys. **113**, 17C725 (2013)
[9] Yongke Yan, Yuan Zhou, and Shashank Priya, Appl. Phys. Lett. **104**, 032911 (2014)
[10] Gaojian Wu, Tianxiang Nan, Ru Zhang, Ning Zhang, Shandong Li, and Nian X. Sun, Appl. Phys. Lett. **103**, 182905 (2013)
[11] Jaydip Das, Young-Yeal Song, and Mingzhong Wu, J. Appl. Phys. **108**, 043911 (2010)
[12] H. K. D. Kim, L. T. Schelhas, S. Keller, J. L. Hockel, S. H. Tolbert, and G. P. Carman, Nano Lett. **13**, 884 (2013).
[13] S. Zhang, Y. G. Zhao, P. S. Li, J. J. Yang, S. Rizwan, J. X. Zhang, J. Seidel, T. L. Qu, Y. J. Yang, Z. L. Luo, Q. He, T. Zou, Q. P. Chen, J. W. Wang, L. F. Yang, Y. Sun, Y. Z. Wu, X. Xiao, X. F. Jin, J. Huang, C. Gao, X. F. Han, and R. Ramesh, Phys. Rev. Lett. **108**, 137203 (2012).
[14] N. D. Mathur and J. F. Scott, Phil. Trans. R. Soc. A **372**, 20120453 (2014).
[15] Zhiguang Wang, Yue Zhang, Ravindranath Viswan, Yanxi Li, Haosu Luo, Jiefang Li, and D. Viehland, Phys. Rev. B. **89**, 035118 (2014).
[16] B. Lorenz, Y. Q. Wang, Y. Y. Sun, and C. W. Chu, Phys. Rev. B **70**, 212412 (2004).
[17] R. C. Rai, J. Cao, J. L. Musfeldt, S. B. Kim, S.-W. Cheong, and X. Wei, Phys. Rev. B **75**, 184414 (2007).
[18] Chan-Ho Yang, Sung-Ho Lee, T. Y. Koo, and Y. H. Jeong, Phys. Rev. B **75**, 140104 (2007).
[19] U. Adem, L. Wang, D. Fausti, W. Schottenhamel, P. H. M. van Loosdrecht, A. Vasiliev, L. N. Bezmaternykh, B. Büchner, C. Hess, and R. Klingeler, Phys. Rev. B **82**, 064406 (2010).
[20] S. Mukherjee, C. H. Chen, C. C. Chou, K. F. Tseng, B. K. Chaudhuri, and H. D. Yang, Phys. Rev. B **82**, 104107 (2010).
[21] S. Kamba, V. Goian, M. Orlita, D. Nuzhnyy, J. H. Lee, D. G. Schlom, K. Z. Rushchanskii, M. Ležaić, T. Birol, C. J. Fennie, P. Gemeiner, B. Dkhil, V. Bovtun, M. Kempa, J. Hlinka, and J. Petzelt, Phys. Rev. B **85**, 094435 (2012).
[22] J. Hwang, E. S. Choi, H. D. Zhou, Y. Xin, J. Lu, and P. Schlottmann, Phys. Rev. B **85**, 224429 (2012).
[23] S. Zhang, X. Dong, Y. Chen, G. Wang, J. Zhu, and X. Tang, Solid State Commun. **151**, 982 (2011).
[24] N. A. Pertsev, S. Prokhorenko, and B. Dkhil, Phys. Rev. B **85**, 134111 (2012).
[25] J. H. Park, H. H. Shin, and H. M. Jang, Phys. Rev. B **77**, 212409 (2008).
[26] V. M. Petrov, G. Srinivasan, M. I. Bichurin, and A. Gupta, Phys. Rev. B **75**, 224407 (2007).
[27] G. Evans, G. V. Duong, M. J. Ingleson, Z. L. Xu, J. T. A. Jones, Y. Z. Khimyak, J. B. Claridge, and M. J. Rosseinsky, Adv. Funct. Mater. **20**, 231 (2010).
[28] J. H. Li, I. Levin, J. Slutsker, V. Provenzano, P. K. Schenck, R. Ramesh, J. Ouyang, and A. L. Roytburd, Appl. Phys. Lett. **87**, 072909 (2005).
[29] M. Liu, X. Li, H. Imrane, Y. J. Chen, T. Goodrich, Z. H. Cai, K. S. Ziemer, J. Y. Huang, N. X. Sun, Appl. Phys. Lett. **90**, 152501 (2007).
[30] R. Liu, Yuzhen Zhao, R. Huang, Yongjie Zhao, and H. Zhou, J. Mater. Chem. **20**, 10665 (2010).
[31] M. T. Buscaglia, V. Buscaglia, L. Curecheriu, P. Postolache, L. Mitoseriu, A. C. Ianculescu, B. S. Vasile, Z. Zhe, and P. Nanni, Chem. Mater. **22**, 4740 (2010).
[32] K. Raidongia, A. Nag, A., Sundaresan, and C. N. R. Rao, Appl. Phys. Lett. **97**, 062904 (2010).
[33] J. B. Tracy and T. M. Crawford, MRS Bull. **38**, 915 (2013).
[34] S. Singamaneni, V. N. Bliznyuk, C. Binek, and E. Y. Tsymbal, J. Mater. Chem. **21**, 16819 (2011).
[35] Y. Yang, S. Priya, J. Li, and D. Viehland, J. Am. Ceram. Soc. **92**, 1552 (2009).
[36] Tien-Kan Chung, Kin Wong, Scott Keller, Kang L. Wang, and Gregory P. Carman, J. Appl. Phys. **106**, 103914 (2009).
[37] G. Caruntu, A. Ypurdkhani, M. Vopsaroiu, and G. Srinivasan, Nanoscale **4**, 3218 (2012).
[38] V. Hong, S. I. Presolski, C. Ma, and M. G. Finn, Angew. Chem. Int. Ed. **48**, 9879 (2009).
[39] A. C. Cardiel, M. C. Benson, L. M. Bishop, K. M. Louis, J. C. Yeager, Y. Tan, and R. J. Hamers, ACS Nano **6**, 310 (2012).
[40] L. M. Bishop, J. C. Yeager, X. Chen, J. N. Wheeler, M. D. Torelli, M. C. Benson, S. D. Burke, J. A. Pedersen, and R. J. Hamers, Langmuir **28**, 1322 (2012).

[41] Gollapudi Sreenivasulu, Maksym Popov, Ferman A. Chavez, Sean L. Hamilton, Piper R. Lehto, and Gopalan Srinivasan, Appl. Phys. Lett. **104**, 052901 (2014).
[42] Landolt-Bornstein; Numerical data and functional relationships in science and technology, Group III, Crystal and Solid State Physics, vol 4(b), *Magnetic and Other Properties of Oxides*, eds. K.-H. Hellwege and A. M. Springer (Springer-Verlag, New York, 1970).
[43] A. M. Nicolson and G. F. Ross, IEEE Trans. Instrum. Meas. **IM-19**, 377–382 (1970).
[44] A. A. P. Gibson, B. M. Dillon, and S. I. Sheikh, Int. J. Electron. **76**, 1073 (1994).
[45] N. Hur, S. Park, P. A. Sharma, S. Guha, and S. W. Cheong, Phys. Rev. Lett. **93**, 107207 (2004).
[46] T. Kimura, T. Goto, H. Shintani, K. Ishizaki, T. Arima, and Y. Tokura, Nature **426**, 55 (2003).
[47] S. Singh, N. Kumar, R. Bhargava, M. Sahni, K. Sung, and J. H. Jung, J. Allyos and Compounds **587**, 437 (2014).
[48] J. X. Zhang, J. Y. Dai, W. Lu, H. L. W. Chan, B. Wu, and D. X. Li, J. Phys. D: Appl. Phys. **41**, 235405 (2008).
[49] J. Zhou, Y. Zhang, G. Zhang, and P. Liu, J. Appl. Phys. **113**, 043907 (2013).
[50] M. A. Popov, I. V. Zavislyak, G. Srinivasan, IEEE Trans. Mag. **47**, 289 (2011).
[51] D. A. G. Bruggeman, Ann. Phys. (Leipsig) **24**, 636 (1935).
[52] Jay G. Liu and David L. Wilcox Sr., J. Appl. Phys. **77**, 6456 (2006).
[53] M. Y. Koledintseva, R. E. Dubroff, and R. W. Schwartz, Progress In Electromagnetics Research, PIER **63**, 223, 2006.
[54] H. Sihvola and I. V. Lindell, J. Electromagnetic Waves Appl. **3**, 37 (1989).
[55] T. N. Yang, Jia-Mian Hu, C. W. Nan, and L. Q. Chen, Appl. Phys. Lett. **104**, 052904 (2014).
[56] J. Petzelt, T. Ostapchuk, A. Pashkin, and I. Rychetsky, J. Euro. Ceram. Soc. **23**, 2627 (2003).
[57] U. Netzelmann, J. Appl. Phys. **68**, 1800 (1990).
[58] J. D. Eshelby, Proceedings of Royal Society A **241**, 376.
[59] M. Bilgen and M. Insana, Phys. Med. Biol. **43**, 1 (1998).
[60] A. G. Gurevich, G. A. Melkov, *Magnetization Oscillations and Waves* (CRC Press, NewYork, 1996).